Three-dimensional Si islands on Si(001) surfaces

Alexander A. Shklyaev* and Masakazu Ichikawa†
Joint Research Center for Atom Technology (JRCAT), Angstrom Technology Partnership (ATP), 1-1-4 Higashi, Tsukuba, Ibaraki 305-0046, Japan

(Received 11 June 2001; published 28 December 2001)

Three-dimensional Si islands with a number density from 10^{12} to 10^{13} cm^{-2} and size of 3–10 nm were grown on Si(001) substrates covered with 0.3-nm-thick SiO_2 layers. The islands were epitaxial to the Si(001) substrate at growth temperatures above 460 °C. They had a hemispherical shape at temperatures between 400 and 570 °C and a pyramidal shape at temperatures from 570 to 640 °C. The SiO_2 layer was completely desorbed during the pyramidal island formation. Competition between SiO_2 decomposition through the reaction of Si adatoms with SiO_2 and attachment of Si adatoms to nucleating islands determines this growth picture. The potential energy barriers for adatom diffusion between areas of SiO_2 and bare Si and at step edges on Si surfaces are also responsible for the hemispherical and pyramidal shapes of the islands, respectively. Estimates showed that island nucleation occurred through the reaction between individual Si adatoms and SiO_2. A dot modification of δ-doped Si layers in Si and also Si dots in a SiO_2 matrix can be created by the present method.

DOI: 10.1103/PhysRevB.65.045307 PACS number(s): 81.07.−b, 68.37.Ef, 68.37.Lp

I. INTRODUCTION

Since the effect of quantum carrier confinement can essentially modify physical properties of materials, in the last decade considerable efforts have been concentrated on methods of creating quantum dot structures with a dot size of the order of 10 nm. Silicon growth on Si substrates normally occurs through the layer-by-layer mode involving nucleation of two-dimensional (2D) islands.[1,2] Such a growth mode was used to create δ-doped layers and wells in a Si matrix.[3] In order to create three-dimensional islands on the base of Si, which can serve as a layer of quantum dots, modification of the growth mode has mostly been performed by introducing a large amount of Ge in the Si deposition flux, thereby creating layers of SiGe dots in a Si matrix.[4,5] The 3D island formation occurred in the growth of SiGe layers to reduce the lattice strain caused by the lattice mismatch between SiGe and Si. However, promising approaches to the formation of nanometer-sized 3D Si islands without Ge have not been invented.

In this work, we used an ultrathin SiO_2 layer as an intermediate coverage on Si(001) substrates prior to Si deposition. Because of inhomogeneous decomposition of the SiO_2 layer through SiO desorption under the flux of Si atoms, the conditions for epitaxial island nucleation and their 3D growth appeared on the areas of bare Si substrate. At low temperatures, when the rate of Si adatom attachment to the growing island was higher than the rate of SiO_2 decomposition, the SiO_2 decomposition was suppressed by the island growth as soon as islands were nucleated. As a result, the rest of the SiO_2 layer remained on the surface even at the later Si deposition stages, acting on the shape of growing 3D Si islands making it hemispherical. At higher temperatures, the SiO_2 could completely desorb and the epitaxial Si islands took a pyramidal shape on the Si(001) substrate.

There is another aspect of the study concerning the formation of Si dots embedded in a SiO_2 matrix. For such structures, stimulated light emission has been detected, which supports the idea of fabricating a silicon laser.[6] The structures have been created by various methods such as Si-ion implantation into SiO_2 (Refs. 6–8), plasma deposition from silane,[9,10] and *e*-beam evaporation of Si combined with plasma activation of an argon-oxygen atmosphere.[11] The results of this work show that the Si 3D island structures can be grown by direct Si deposition on the SiO_2 layer. The islands had a density of the order of 10^{12}–10^{13} cm^{-2} and a size of 3–10 nm, which was determined by the amount of Si deposited. By alternating oxidation and Si deposition, the structure of Si dots in a SiO_2 matrix can be created with controllable parameters such as the thickness of the SiO_2 layers and the size of Si dots.

II. EXPERIMENT

The experiments were carried out in an ultrahigh-vacuum (UHV) chamber with a base pressure of about 1×10^{-10} Torr. The chamber was equipped with a STM and a UHV field-emission scanning-electron-microscope (SEM) gun, a microprobe reflection high-energy electron diffraction (μ-RHEED) detector, and a secondary-electron detector. The scanning reflection electron microscopy (SREM) images were formed using a glancing angle of the electron beam on the sample surface of about 2° at the 30-kV accelerating voltage. This glancing angle was also used to obtain RHEED patterns from the sample surface. The STM apparatus was specially developed to be combined with the SEM gun. The condition of the W tip and manipulations with the tip on the Si surface were monitored with the SREM. The STM images were usually obtained with a tip bias voltage of either −3.0 or −4.0 V and a constant current between 0.15 and 0.3 nA. Details of the apparatus have been described elsewhere.[12]

A $12\times1.5\times0.4$-mm sample was cut from an *n*-type Si(001) wafer with a miscut angle of $<1'$ and a resistivity of 5–10 Ω cm. Clean Si surfaces were prepared by flash direct-current heating at 1200 °C. To oxidize the surface, we raised

the sample temperature from room temperature to 640 °C for 10 min after oxygen had been introduced into the chamber at a pressure of 2×10^{-6} Torr. The thickness and chemical composition of the oxide layers were characterized by producing oxide layers under the same conditions in a separate x-ray photoelectron spectroscopy system.[13] The layer thickness was estimated to be 0.3 nm and the oxide layers were mainly composed of silicon dioxide (SiO_2). A high-temperature Knudsen cell with a graphite crucible was used to deposit Si at a deposition rate of 0.5 ML/min [1 monolayer (ML) $=6.78\times10^{14}$ atoms/cm^2], which was calibrated by measuring the period of specular spot RHEED intensity oscillations during layer-by-layer growth on Si(111) substrates.[14] The growth temperature was set 0.5 min before starting the Si deposition and was maintained for 0.3 min after finishing the deposition.

III. RESULTS AND DISCUSSION

Silicon homoepitaxy usually occurs through nucleation of 2D islands on the terraces between the steps and layer-by-layer growth.[1,2] By introducing the ultrathin oxide layer on the Si surface, the Si growth mode was dramatically modified: the deposited Si appeared as 3D islands whose shape was dependent on the growth temperature. At temperatures between 400 and 570 °C, the islands had a semispherical shape, as shown in Figs. 1(a) and 1(b). At high temperatures from 570 to 640 °C, the islands were four-sided pyramids [Figs. 1(c) and 1(d)]. The structure of the islands was also dependent on the growth temperature, as can be discerned from the RHEED patterns shown in Fig. 2. The RHEED patterns obtained after Si deposition at temperatures above 460 °C contained bright spots indicating electron diffraction from 3D islands epitaxially growth on the Si(001) substrate. These diffraction spots gradually became weaker and then disappeared in the RHEED patterns as the growth temperature decreased to 400 °C. This indicates that the number of epitaxially grown islands decreased with decreasing temperature, and at 400 °C, the islands were mostly grown nonepitaxially.

The bare Si areas required for epitaxial island formation can appear due to a reaction between the deposited Si and the SiO_2 layer. The RHEED data showed that nonepitaxial islands grown at 400 °C did not transform into epitaxial islands after annealing at 500 °C for 10 min. This postdeposition annealing experiment implies that the reaction between Si and SiO_2 for epitaxial island formation did not occur at the island-SiO_2 interfaces, but occurred between Si adatoms and SiO_2 at the initial stage of Si deposition, that is, before the adatoms were incorporated into islands. The areas of bare Si can thus appear at elevated temperatures through the reaction

$$\mathrm{SiO_2}(s)+\mathrm{Si}(ad)\rightarrow 2\,\mathrm{SiO}(g). \quad (1)$$

In the case of O_2 adsorption on clean Si surfaces, the desorption of SiO molecules was observed at temperatures as low as 500 °C through the reaction[15,16]

$$2\,\mathrm{Si}(s)+\mathrm{O_2}(ad)\rightarrow 2\,\mathrm{SiO}(g). \quad (2)$$

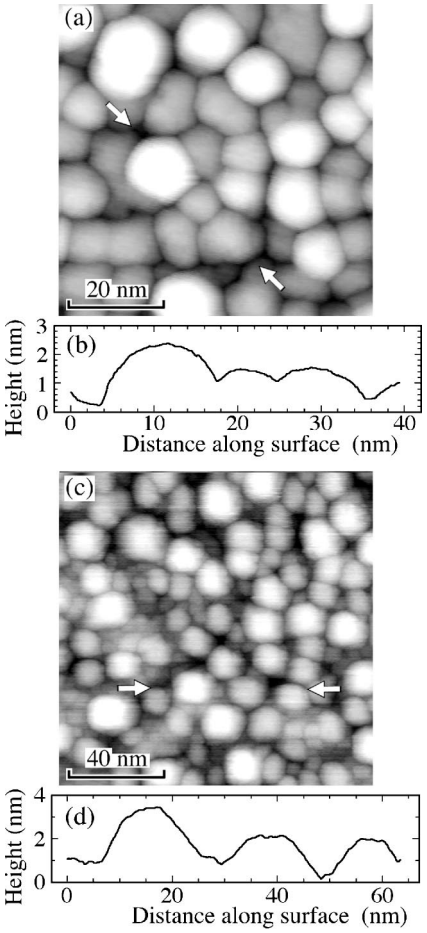

FIG. 1. STM data for Si islands appearing after 5.8-ML Si deposition on Si(001) surfaces covered with 0.3-nm-thick SiO_2 layers. The growth temperature was 420 °C in (a) and 590 °C in (c). (b) and (d) Height profiles between arrows marked in (a) and (c), respectively. The orientations of facets on the sidewalls in (c) were mostly {113} and {115}.

Reactions (1) and (2) describe SiO desorption on SiO_2 and Si surfaces, respectively. The epitaxial Si island growth which follows SiO_2 decomposition indicates that the formation of volatile SiO molecules through reaction (1) can occur at temperatures of 420–460 °C, which are even lower than the temperatures for SiO desorption through reaction (2).

The hemispherical shape of Si islands is natural on SiO_2 surfaces when the bonds between atoms in the islands are

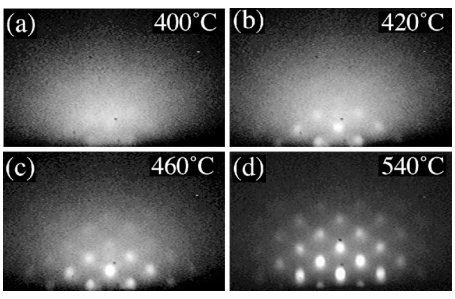

FIG. 2. RHEED patterns of Si islands grown by 5.8-ML Si deposition on Si(001) surfaces covered with 0.3-nm-thick SiO_2 layers. The growth temperatures are shown in the patterns.

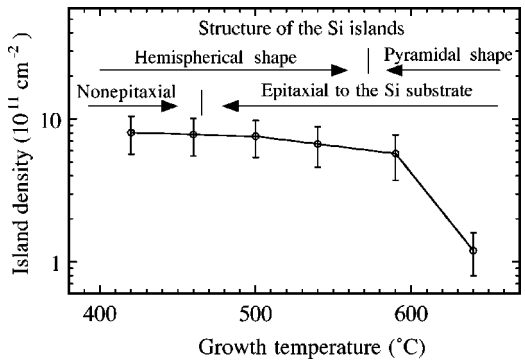

FIG. 3. Temperature dependence of the island density for islands grown by 5.8-ML Si deposition on Si(001) surfaces covered with 0.3-nm-thick SiO_2 layers. To count the islands, they were taken as separated from each other if the valleys between them in the STM images were deeper than half their height.

significantly stronger than those between atoms of the islands and atoms of the substrate. However, such a shape observed at growth temperatures between 460 and 570 °C is not typical for epitaxial islands. Formation of the hemispherical epitaxial islands reflects competition between reaction (1) and the reaction of Si adatom attachment to the growing islands: After the appearance of island nucleation centers due to the reaction (1), the reaction of Si adatom attachment to the growing islands dominates reaction (1). As a result, the islands grow in the radial direction over the rest of the SiO_2 layer, burying it under the islands. This effect has been observed with a transmission electron microscope for hemispherical Ge island formation on oxidized Si(111) surfaces.[17] Therefore, the epitaxial growth of the hemispherical Si islands is determined by the epitaxial nature of island nucleation at the initial stage of Si deposition. This implies that the hemispherical epitaxial islands were bound to the Si only in the nucleation areas of the island-substrate interface. Whereas, Si atoms at the edges of the islands were bound more weakly to the rest of the SiO_2 film. These bonding conditions were close to those of islands on SiO_2 surfaces and therefore determined the hemispherical shape of the Si islands. Interestingly, in spite of the differences in shape and structure, the islands had a density which was almost independent of temperature from 400 to 590 °C, as shown in Fig. 3. Since islands touched each other and coalesced, we counted them based on a criterion: the islands were considered to be separated if the depth of valleys between them was larger than 50% of their heights. We took into account that the real depth of valleys between the islands was larger than that observed in the STM images because of the effect of the STM tip size on the image of the foot of islands, particularly when the islands had a hemispherical shape.

At growth temperatures above 570 °C, the Si islands had {113}, {115}, and {117} facets on the sidewalls, which formed four-sided pyramids. To produce conditions for the pyramid formation, reaction (1) must occur quickly enough to create areas of bare Si around the growing islands. However, the increasing SiO_2 decomposition rate with temperature also caused a decrease in island density, as shown in Fig. 3, indicating a weakening of the effect of inhomogeneous decomposition of the SiO_2 layer on 3D island formation. At the same time, with the decreasing island density, some of the Si islands grew up to 30 nm in base length and had well-formed {117} facets on the sidewalls, as shown in Fig. 4. The STM images obtained after island formation at the high growth temperatures (Fig. 4) clearly showed (001) terraces and atomic steps between the pyramidal Si islands without the presence of the rest of the SiO_2 layer. Schemes of the surface structures for various temperatures are shown in Fig. 5.

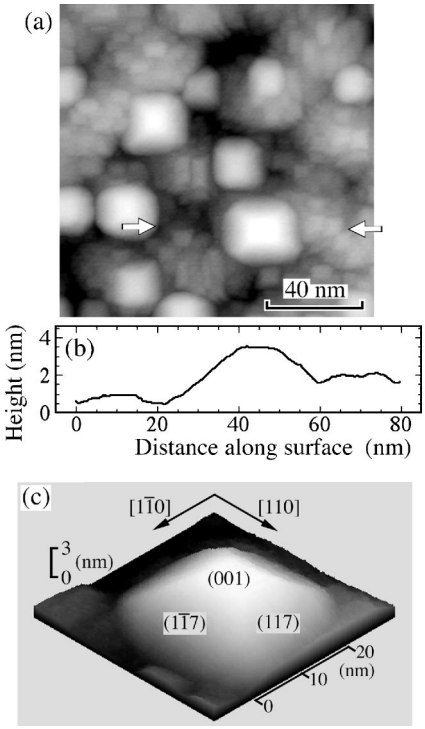

FIG. 4. STM data of pyramidal Si islands with the {115} and {117} facets on the sidewalls. The islands were grown by 5.8-ML Si deposition on Si(001) surfaces covered with 0.3-nm-thick SiO_2 layers. The growth temperature was 640 °C. (b) Height profile between arrows marked in (a). (c) STM image of a relatively large Si island.

Three-dimensional Si islands are usually thermally unstable on Si surfaces. However, under the Si deposition flux, thermally generated adatoms and adatoms deposited by the flux created nonequilibrium kinetic conditions at which the growth of pyramidal islands dominated their decay. At high temperatures, the rest of SiO_2 films on the surface between

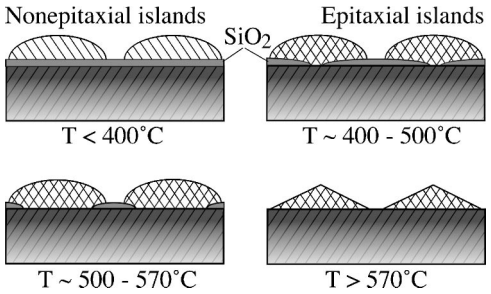

FIG. 5. Sketch of surface structures for various growth temperatures.

the pyramidal islands could continue the decomposition even after the island nucleation, producing new surface areas of bare Si. These areas attached Si adatoms resulting in the formation of small terraces and irregular atomic steps containing many step kinks, as one can see in Fig. 4(a). Such surfaces can thermally generate Si adatoms with high density around the pyramidal islands. This adatom density must be much higher than that around a single Si island on atomically flat Si surfaces.[18] It is expected that this kinetic factor can significantly reduce the rate of flattening of the surface morphology after closing the deposition flux, when migration of thermally generated Si adatoms only determines the formation of equilibrium surface morphology.

Formation of four-sided pyramids is usual on a surface such as Si(001). For example, the so-called hut islands with {015} facets on the sidewalls appear in the epitaxy of Ge on Si(001) surfaces.[19] The clean Si surfaces oriented under certain angles to the (001) plane exhibit a sequence of energetically stable surface orientations, $\{1,1,2n+1\}$, where $n=1,2$, etc.[20] Such orientations were also observed for facets on the sidewalls of Si pyramids grown by low pressure chemical vapor deposition[21] and ultrahigh-vacuum thermal decomposition of Si_2H_6 (Ref. 22) in the restricted areas of Si(001) windows in SiO_2 films. The slope angle of the sidewalls increased, which corresponded to the transformation from {1,1,13} to {113} facets, when the pyramids grew to 50 nm in the lateral dimension.[22] In our case, the islands that were small in the lateral dimension usually had {113} and {115} facets on the sidewalls. The orientation of facets varied through {115} to {117} as the islands became larger in base length. The shape of the islands was not in equilibrium as it was in the cases of Refs. 21 and 22. Instead, simultaneous processes such as island growth under the Si flux, island decay, and inhomogeneous decomposition of the rest of the SiO_2 layer between the islands determined the dynamic conditions for the formation of island shape in our case.

For the hemispherical islands, the number density of islands was dependent on the amount of deposited Si, as shown in Fig. 6. The density reached a maximum of approximately 10^{13} cm^{-2} at a Si coverage of about 0.7 ML (Fig. 7), at which the islands created were about 3 nm in base length. When the Si coverage increased, the density gradually decreased because of coalescence through overgrowth of nearby islands. It is to be noted that after the creation of the layer of 3D Si islands at 400 °C at which the SiO_2 decomposition did not occur, the conditions for growing the second layer of the islands were obtained by subsequent oxidation in oxygen. Repeated application of this method allows the fabrication of a structure of Si islands in a SiO_2 matrix. The island size and the thickness of the SiO_2 layer between islands are controllable through the amount of Si deposited and the oxidation conditions, respectively. The islands can be given a diameter of about 3 nm and a density of the order of 10^{19} cm^{-3}, which can likely produce the stimulated light emission.[6]

At small coverages (before coalescence of islands), the density of islands is determined by the mechanism of island nucleation. The obtained data show that the density was almost independent of the growth temperature in the range between 400 and 590 °C (Fig. 3), and the density was approximately the same for the hemispherical and pyramidal islands. The creation of both chemically active SiO(s) states for nonepitaxial island formation by breaking Si-O bonds of SiO_2 and areas of bare Si for epitaxial island formation through SiO(g) desorption at high temperatures can occur due to the reaction

$$SiO_2(s)+Si(ad)\rightarrow SiO(s)+SiO(g). \tag{3}$$

The relation between the SiO(s) and SiO(g) products is a function of temperature. The density of islands can be estimated on the assumption that the nucleation centers for islands appear due to reaction (3). The distance d between islands is given by the average diffusion length x of Si adatoms on the SiO_2 surface $d=2x$. The diffusion length is[23]

$$x=(D\tau_r)^{1/2}, \tag{4}$$

where $D=\nu a^2\exp(-E_d/kT)$ is the diffusion coefficient of Si adatoms on the SiO_2 surface, ν is the frequency factor ($\nu\approx10^{13}$ s^{-1}), a is the jump distance ($a\approx0.3$ nm) of the

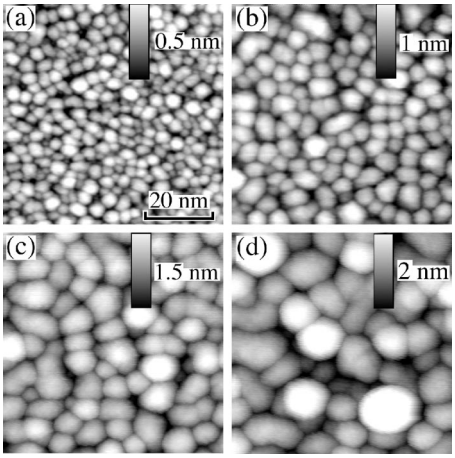

FIG. 6. STM images of Si islands grown by deposition of various amount of Si on Si(001) surfaces covered with 0.3-nm-thick SiO_2 layers. The growth temperature was 400 °C. The Si coverages were 0.7 ML in (a), 1.4 ML in (b), 4.6 ML in (c), and 5.8 ML in (d). All images show areas of the same size of 66×66 nm^2.

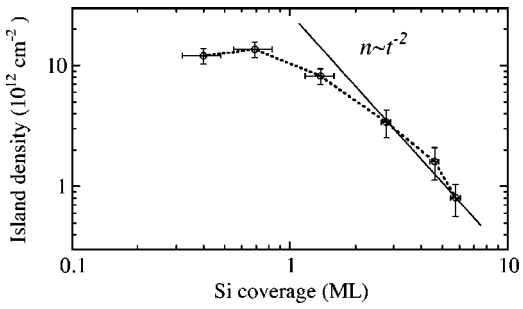

FIG. 7. Density of Si islands as a function of Si coverage. The growth conditions were the same as those in Fig. 6. The solid line represents the approximation of the density by the power function $n\sim t^{-2}$, where the coverage is proportional to the growth time t at a constant Si deposition rate.

order of the surface repeat distance, E_d is the diffusion activation energy, and τ_r is the lifetime of Si adatoms on the surface, determined by the rate of reaction (3), $\tau_r^{-1} = k_r^{(o)}\exp(-E_r/kT)$, where $k_r^{(o)}$ is the prefactor of the reaction rate constant and E_r is the activation energy of the reaction (3). Since the density n is $n=d^{-2}$, we obtain

$$n=[k_r^{(o)}/(4\nu a^2)]\exp[(E_d-E_r)/kT]. \quad (5)$$

That the density is almost independent of temperature in the range from 400 to 590 °C suggests $E_d \approx E_r$. At $n \approx 10^{13}$ cm^{-2}, Eq. (5) gives a value of $k_r^{(o)}=3.6\times10^{-2}$. This value is reasonable for reactions of individual adatoms with atoms of the surface, where $k_r^{(o)}$ is usually smaller than ν by a factor of the order of 10^{-2} (Ref. 24). The corresponding average diffusion length is $x \approx 1.6$ nm. The nucleation at which an individual adatom becomes a stable nucleus through reaction with an atom on the surface corresponds to a growth model with the critical island size $i^*=0$. It is to be noted that expressions for n similar to Eq. (5) have been derived in various studies of nucleation occurring at saturated adatom densities maintained by the balance between deposition and fast adatom desorption.[25,26] Schmidt *et al.* observed a high number density such as 10^{13} cm^{-2} for clusters of some metals deposited on SiO_2 substrates.[27] They suggested the existence of correlation in which the density is higher for metals whose heat of sublimation on SiO_2 is greater. Our results show that the density of Si islands is about five times larger than that of Ge islands on SiO_2 (Ref. 28) and this large difference cannot be related to the difference in heats of sublimation for Si and Ge. Since the Si and Ge islands on SiO_2 were grown at the conditions of complete condensation, the observed difference in densities is determined by the difference in chemical reactivity of Si and Ge adatoms on SiO_2.

For metals, the step edge barrier (the Ehrlich-Schwoebel barrier[29,30]) for diffusion usually determines the evolution of 3D surface morphology in epitaxy. In our case, after Si island nucleation, another potential energy barrier appears. This barrier is between areas of SiO_2 and bare Si on the islands. The barrier has a value of about 3 eV (Ref. 31) and also causes the development of the surface morphology. This barrier along with the difference in the bonding conditions between atoms in the islands and at the island-SiO_2 interfaces is responsible for the hemispherical shape of islands. In the presence of SiO_2 between the islands, the coalescence of islands occurs through the overgrowth mechanism when the nearby islands start to coalesce after the SiO_2 is completely covered with the growing islands. Therefore the SiO_2 preserves valleys between the islands for the later stage of island growth than that by the Schwoebel barrier. For such conditions, the surface morphology can be characterized by the density of islands even at coverages much above the jamming limit, as used in Figs. 3 and 6. The island density as a function of the growth time can be derived in a simple model on the assumption that the islands are uniform at each coverage. The amount V of Si deposited is $V=wt$, where w and t are the deposition rate and time, respectively. On the other hand, the deposited Si is mostly spent on the island formation, that is, $V=n\rho$, where n is the island density and ρ is the island volume, if all islands have an equal size. When the Si coverage is larger than the jamming limit, there is no free space between the islands, $n=1/s$, where s is the area of an island on the surface. Since $s\sim\rho^{2/3}$, $\rho\sim n^{-3/2}$, hence we obtain $V=wt\sim n^{-1/2}$ or $n\sim t^{-2}$. The approximation of experimental data by the power function for the island density at coverages above the jamming limit is shown in Fig. 7.

At growth temperatures above 570 °C, the islands were pyramidal and well separated from each other, as shown in Figs. 1(c) and 4(a), and none of the rest of the SiO_2 layer was observed on the Si(001) surface between the islands. The 3D Si islands were nucleated at the initial stage of Si deposition due to inhomogeneous decomposition of the SiO_2 layer. However, the islands did not decay during further Si deposition when the SiO_2 layer had been completely desorbed. This behavior is different from that observed for Ge deposited on the SiO_2 layer on the Si substrate.[28] At high temperature, the SiO_2 layer can also completely decompose under the flux of Ge atoms through volatile SiO and GeO formation. Under similar conditions, Ge had a tendency to form a wetting layer on the Si substrate. This difference between Si and Ge implies that the effect of the decreasing surface free energy by flattening the surface morphology acts stronger for 3D Ge islands on Si surfaces (at Ge coverages smaller than the critical coverage of the 2D-3D growth transition) than for 3D Si islands on Si surfaces. This allows the creation of, for example, a layer of doped Si dots in an undoped Si matrix if a dopant is introduced at the stage of 3D Si island formation and the islands are then covered with an undoped Si layer. By alternating such Si growth with Si oxidation, a multiplayer structure of doped Si dots in a Si matrix can be fabricated.

IV. CONCLUSIONS

Inhomogeneous decomposition of ultrathin SiO_2 layers on a Si (001) substrate under the flow of Si atoms created areas of bare Si substrate, which served as centers for epitaxial nucleation and growth of 3D Si islands. At high temperatures from 590 to 640 °C, the SiO_2 layer could completely desorb through reaction with Si adatoms, and the epitaxial 3D Si islands appeared, which had a pyramidal shape with {113}, {115}, and {117} facets on the sidewalls on the Si(001) surface. At temperatures between about 460 and 570 °C, the epitaxial islands had a hemispherical shape, which indicated incomplete desorption of the SiO_2 layer. At temperatures about 400 °C, the hemispherical islands were nonepitaxial to the Si(001) substrate, so they were separated from the substrate by the SiO_2 layer. The experimental results suggest that the island nuclei and the conditions for epitaxial growth appear through a reaction between individual Si adatoms and SiO_2, and the mechanism of island nucleation corresponds to a growth model with the critical island size $i^*=0$. The high reactivity of Si adatoms on SiO_2 provides a high nucleation density of the order of 10^{13} cm^{-2} for 3D Si islands. Our results show the possibilities of creating (1) layers of Si dots in a SiO_2 matrix with a high dot density of the order of

10^{19} cm^{-3}, which is interesting for light emission studies and (2) layers of doped Si dots in a Si matrix by Si deposition at temperatures of complete SiO_2 decomposition; these layers can be treated as a dot modification of δ-doped Si layers and wells in Si.

This work, partly supported by the New Energy and Industrial Technology Development Organization (NEDO), was carried out at JRCAT under an agreement between the National Institute for Advanced Industrial Science and Technology (AIST) and ATP.

*On leave from the Institute of Semiconductor Physics, Novosibirsk, 630090, Russia.

†Electronic address: ichikawa@jrcat.or.jp

[1] T. Sakamoto, N. J. Kawai, T. Nakagawa, K. Ohta, and T. Kojima, Appl. Phys. Lett. **47**, 617 (1985).

[2] Y.-W. Mo, B. S. Swartzentruber, R. Kariotis, M. B. Webb, and M. G. Lagally, Phys. Rev. Lett. **63**, 2393 (1989).

[3] H. J. Gossmann and E. F. Schubert, CRC Crit. Rev. Solid State Mater. Sci. **18**, 1 (1993).

[4] C. Teichert, M. G. Lagally, L. J. Peticolas, J. C. Bean, and J. Tersoff, Phys. Rev. B **53**, 16 334 (1996).

[5] W. Dorsch, H. P. Strunk, H. Wawra, G. Wagner, J. Groenen, and R. Carles, Appl. Phys. Lett. **72**, 179 (1998).

[6] L. Pavesi, L. Dal Negro, C. Mazzoleni, G. Franzo, and F. Priolo, Nature (London) **408**, 440 (2000).

[7] S. Guha, M. D. Pace, D. N. Dunn, and I. L. Singer, Appl. Phys. Lett. **70**, 1207 (1997).

[8] T. S. Iwayama, S. Nakao, and K. Saitoh, Appl. Phys. Lett. **65**, 1814 (1994).

[9] D. Zhang, R. M. Kolbas, P. D. Milewski, D. J. Lichtenwalner, A. I. Kingon, and J. M. Zavada, Appl. Phys. Lett. **65**, 2684 (1994).

[10] S. Tong, X. N. Liu, and X. M. Bao, Appl. Phys. Lett. **66**, 469 (1995).

[11] S. Cheylan, R. G. Elliman, K. Gaff, and A. Durandet, Appl. Phys. Lett. **78**, 1670 (2001).

[12] S. Maruno, H. Nakahara, S. Fujita, H. Watanabe, Y. Kusumi, and M. Ichikawa, Rev. Sci. Instrum. **68**, 116 (1997).

[13] H. Watanabe and M. Ichikawa, Rev. Sci. Instrum. **67**, 4185 (1996).

[14] M. Ichikawa and T. Doi, Appl. Phys. Lett. **50**, 1141 (1987).

[15] N. Shimizu, Y. Tanishiro, K. Kobayashi, K. Takayanagi, and K. Yagi, Ultramicroscopy **18**, 453 (1985).

[16] A. A. Shklyaev, M. Aono, and T. Suzuki, Surf. Sci. **423**, 61 (1999).

[17] A. V. Kolobov, A. A. Shklyaev, H. Oyanagi, P. Fons, S. Yamasaki, and M. Ichikawa, Appl. Phys. Lett. **78**, 2563 (2001).

[18] A. Ichimiya, Y. Tanaka, and K. Ishiyama, Phys. Rev. Lett. **76**, 4721 (1996).

[19] Y.-W. Mo, D. E. Savage, B. S. Swartzentruber, and M. G. Lagally, Phys. Rev. Lett. **65**, 1020 (1990).

[20] B. Z. Olshanetsky and A. A. Shklyaev, Surf. Sci. **82**, 445 (1979); B. Z. Olshanetsky and V. I. Mashanov, *ibid.* **111**, 414 (1981).

[21] L. Vescan, K. Grimm, and C. Dieker, J. Vac. Sci. Technol. B **16**, 1549 (1998).

[22] M. Shibata, Y. Nitta, K. Fujita, and M. Ichikawa, J. Cryst. Growth **220**, 449 (2000).

[23] B. Lewis and D. S. Campbell, J. Vac. Sci. Technol. **4**, 209 (1967).

[24] W. H. Weinberg, in *Kinetics of Interface Reactions*, edited by N. Grunze and H. J. Kreuzer (Springer-Verlag, New York, 1987), p. 94.

[25] D. R. Frankl and J. A. Venables, Adv. Phys. **19**, 409 (1970).

[26] C. T. Campbell, Surf. Sci. Rep. **27**, 1 (1997).

[27] A. A. Schmidt, H. Eggers, K. Herwig, and R. Anton, Surf. Sci. **349**, 301 (1996).

[28] A. A. Shklyaev, M. Shibata, and M. Ichikawa, Phys. Rev. B **62**, 1540 (2000).

[29] G. Ehrlich and F. G. Hudda, J. Chem. Phys. **44**, 1039 (1966).

[30] R. L. Schwoebel and E. J. Chipsey, J. Appl. Phys. **37**, 3682 (1966); R. L. Schwoebel, *ibid.* **40**, 614 (1969).

[31] M. Shibata, Y. Nitta, K. Fujita, and M. Ichikawa, Phys. Rev. B **61**, 7499 (2000).